Technique and Technology
of Land Transport in Construction

DOI: 10.23968/2500-0055-2021-6-4-72-79

DISTRIBUTION OF THE NORMAL REACTIONS ON THE QUANTOMOBILE WHEELS

Jurij Kotikov

Saint Petersburg State University of Architecture and Civil Engineering
Vtoraja Krasnoarmeyskaya st., 4, Saint Petersburg, Russia

E-mail: cotikov@mail.ru

Abstract

Introduction: The progress of science has made it possible to create new quantum engines (QEs) powered by physical vacuum energy. A QE will generate a vector-based propulsive force, or thrust, applicable to the vehicle body directly, with no transmission required. Traditional cars will be upgraded with QEs and thus converted into quantomobiles. QE thrust application at the point of the vehicle body, hovering above the bearing surface, introduces changes in the traditional diagram of forces acting on the vehicle. Therefore, it is necessary to assess the influence of thrust on the longitudinal stability of the quantomobile. **Methods:** In the course of the study, we upgraded the diagram of forces acting on the traditional vehicle, by introducing QE thrust (bearing in mind vehicle hovering above the bearing surface). We also developed a corresponding mathematical model for the distribution of the normal reactions on the wheels, taking into account QE placement. **Results:** Among the developed calculation complexes to perform a qualitative analysis of the influence of force factors on the quantomobile chassis load, a complex representing the longitudinal thrust and the thrust height was distinguished. **Discussion:** These complexes may serve as the basis of calculation units for more detailed programming, analysis, and synthesis of the design of vehicles with QEs, assessment of the longitudinal stability of the vehicle, optimization of QE placement in the quantomobile body. **Example:** The method developed is presented using a quantomobile similar to a KamAZ-4326 automobile. **Conclusion:** The considered diagram of forces acting on a quantomobile, including QE thrust above the bearing surface, shall become generic for force diagrams of quantomobiles with additional thrusters intended to increase the longitudinal stability of the vehicle.

Keywords

Quantum engine, quantomobile, force balance, wheel normal reactions, longitudinal stability

Introduction

The progress of science has created prerequisites for the emergence of entirely new propulsion systems – quantum engines (QEs). The implementation of advanced ideas – e.g., Leonov's quantum engine (Leonov, 2002, 2010) – will make it possible to extract energy from the physical vacuum, by using vehicle power units. A new generation of vehicles with quantum engines – quantomobiles – will replace automobiles (Kotikov, 2018c).

A QE will generate a vector-based propulsive force, or thrust, applicable to the vehicle body directly, with no transmission required (Kotikov, 2018a, 2018c; Leonov, 2010). The wheeled chassis will lose its function as a propulsion unit but will remain a support in the ground movement of the quantomobile (Kotikov, 2019a, 2019b, 2019d, 2019e, 2020). All wheels will become driven.

QE thrust application at the point of the vehicle body, hovering above the bearing surface, introduces changes in the traditional diagram of forces acting on the vehicle. The points of thrust emergence (application) in the wheel contact patches within traditional kinematic diagrams will move towards the points of QE (thruster) thrust vector application to the vehicle body. The vehicle body may have several thrusters.

On the threshold of QE introduction, it is required to develop corresponding kinematic diagrams, which will be quite useful at the early stages of designing quantomobiles and their structural subclasses. The paper addresses the generic scheme of quantomobile movement along the inclined bearing surface where the QE generates longitudinal thrust only. We focus on methodological developments regarding the assessment of the overturning moment caused by QE thrust and assurance of the longitudinal stability of the quantomobile.

Analysis of the normal reactions on the quantomobile wheels

By using the diagram for the determination of the normal reactions R_z on the automobile wheels, presented by Volkov (2018), but in Selifonov's notation (Selifonov et al., 2007), we will consider its transformation for the quantomobile. Figure 1 shows the following: V_q – the velocity vector when moving along a section of the bearing surface (at an angle α to the horizon); C_g – the vehicle center of gravity (CoG); G_q and G_q' – the gravity force and its projection onto the vertical axis of the vehicle; F_{Tx}, F_w, F_j, F_α, F_{f1}, and F_{f2} – the QE longitudinal thrust, wind resistance, reduced vehicle inertia force, climbing force, resistance against the rolling of the front and rear wheels, respectively; T_{f1} and T_{f2} – the rolling resistance moments; h_w, h_{FTx}, h_g – the distance of the vectors of the corresponding forces F_w, F_{Tx}, F_j, and F_α from the bearing surface; L, L_1, and L_2 – the wheelbase and the distance from the wheel axles to the CoG projection onto the bearing surface; A and B – the central points of the contact patches; R_{z1} and R_{z2} – the normal reactions to be determined; Q – the point of QE thrust application to the vehicle body.

The sum of the moments with respect to point B of the rear wheels is as follows:

$$\begin{aligned}&\sum T_B = R_{z1}\cdot L + G_q\cdot \sin\alpha\cdot h_g + m'\cdot\alpha\cdot h_g + \\ &0.5\cdot c_x\cdot\rho\cdot S_{front}\cdot V_q^2\cdot h_w - G_q\cdot\cos\alpha\cdot L_2 + \\ &T_{f1}+T_{f2}-F_{Tx}\cdot h_{FTx}=0,\end{aligned} \quad (1)$$

where:

c_x – the wind shape coefficient;

ρ – the air density, kg/m³;

S_{front} – the frontage area of the quantomobile, m²;

m' – the reduced vehicle mass (with account for the rotational inertia of the wheels), kg;

a – the acceleration of the quantomobile, m/s².

For the reduced vehicle mass, the following is true: $m' = m\cdot\delta_{ric} = (G_q/g)\cdot\delta_{ric}$, where δ_{ric} – the rotational inertia coefficient of the wheels. In the case of quantomobiles, this coefficient takes into account only the rotation of the carrying wheels since there are no rotating power drive parts (an ICE with a flywheel, a clutch coupling, a gearbox, a final drive).

Let us take into account that $T_{f1} + T_{f2} = f R_{z1} r_d + f R_{z2} r_d = (R_{z1} + R_{z2}) f r_d = G_q \cos\alpha f r_d$, where r_d – the dynamic radius of the wheel. In this section, we will not reveal the structure of the coefficient of resistance to the rolling of the wheels f, bearing in mind that it represents the velocity function.

Based on the sum of the moments (1), R_{z1} can be expressed as follows:

$$R_{z1} = \frac{G_q\cdot L_2}{L}\left(\begin{array}{l}(\cos\alpha - \frac{h_g}{L_2}\cdot\sin\alpha) - (\frac{c_x\cdot\rho\cdot S_{front}\cdot V_q^2}{2\cdot G_q\cdot L_2}\cdot h_w) \\ -(\frac{a}{g}\cdot\frac{h_g}{L_2}\cdot\delta_{ric}) - (\cos\alpha\cdot f\cdot\frac{r_d}{L_2}) + (\frac{F_{Tx}\cdot h_{FTx}}{G_q\cdot L_2})\end{array}\right). \quad (2)$$

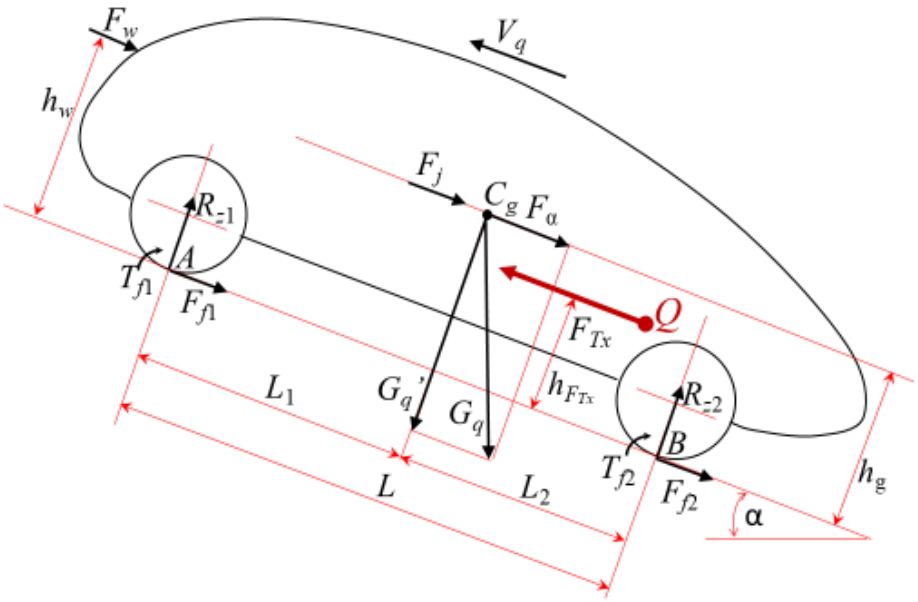

Figure 1. A computational model for the normal reactions on the quantomobile wheels

It seems that the following form will be more convenient in the analysis of the quantomobile configuration:

$$R_{z1} = \frac{G_q}{L}\left(\begin{array}{c}(\cos\alpha(L_2 - f\cdot r_{\ddot{a}}) - h_g\cdot\sin\alpha) - \\ (\frac{c_x\cdot\rho\cdot S_{front}\cdot V_q^{\,2}}{2\cdot G_q}\cdot h_w) - \\ (\frac{a}{g}\cdot h_g\cdot\delta_{ric}) + (\frac{F_{Tx}\cdot h_{FTx}}{G_q})\end{array}\right) = \quad (3)$$

$$= \frac{G_q}{L}(k_{\omega n2} - k_{wn} - k_{jn} + k_{FTxn}).$$

Here, we introduce notations (that differ significantly from Selifonov's notation (Selifonov et al., 2007) for the complexes having the length dimension, each of which represents a share in the shift of the center of dynamic equilibrium in the normal reactions of the vehicle axles.

$k_{\psi n2} = (\cos\alpha(L_2 - f\cdot r_{\ddot{a}}) - h_g\cdot\sin\alpha)$ – the complex of values, describing the interaction between the wheels and the bearing surface. In the case of a horizontal bearing surface, it is reduced to the following: $k_{\psi n2} = (L_2 - f\cdot r_{\ddot{a}})$, where $f\cdot r_d$ represents the shift of the point of dynamic equilibrium from the GoG projection on the bearing surface (due to the presence of the rolling resistance moments T_{f1} and T_{f2}).

$k_{wn} = (\frac{c_x\cdot\rho\cdot S_{front}\cdot V_q^{\,2}}{2\cdot G_q}\cdot h_w)$ – the complex taking into account the influence of wind resistance on the normal reactions;

$k_{jn} = (\frac{a}{g}\cdot h_g\cdot\delta_{ric})$ – the complex taking into account the influence of the longitudinal acceleration of the vehicle on the normal reactions;

$k_{FTxn} = (\frac{F_{Tx}\cdot h_{FTx}}{G_q})$ — the complex taking into account the value of the QE longitudinal thrust and its height relative to the bearing surface.

The same holds for R_{z2} reaction but using the sum of the moments with respect to point *A*. Thus, we will obtain the following for R_{z2}:

$$R_{z2} = \frac{G_q}{L}\left(\begin{array}{c}(\cos\alpha(L_1 + f\cdot r_{\ddot{a}}) + h_g\cdot\sin\alpha) \\ +(\frac{c_x\cdot\rho\cdot S_{front}\cdot V_q^{\,2}}{2\cdot G_q}\cdot h_w) + \\ (\frac{a}{g}\cdot h_g\cdot\delta_{ric}) - (\frac{F_{Tx}\cdot h_{FTx}}{G_q})\end{array}\right) = \quad (4)$$

$$= \frac{G_q}{L}(k_{\omega n1} + k_{wn} + k_{jn} - k_{FTxn}).$$

Let us note that the representation of the result of the interaction between the second axle wheels and an inclined bearing surface differs from the previous one:

$k_{\psi n1} = (\cos\alpha(L_1 + f\cdot r_{\ddot{a}}) + h_g\cdot\sin\alpha)$.

Discussion

The $k_{\psi n1}$, $k_{\psi n2}$, k_{wn}, k_{jn}, k_{FTxn} coefficients represent convenient complexes for qualitative analysis of the influence of force factors on the quantomobile chassis load. These complexes have the length dimension (m) and represent the shift of the point of dynamic equilibrium of the normal reactions along the wheelbase L (let us call them linear complexes). They may serve as the basis of calculation units for more detailed programming, analysis, and synthesis of the design of vehicles with QEs, assessment of the overturning moment, optimization of QE placement in the quantomobile body.

The $k_{FTxn} = (\frac{F_{Tx}\cdot h_{FTx}}{G_q})$ complex in Eqs. (3) and (4) is of particular interest since it describes the force leading to the vehicle nosedive (emergence of the longitudinal overturning moment of forces), which is directly proportional to QE thrust and its height. If we remove the parentheses in Eq. (3) and analyze the $R_{s1} = \ldots + \frac{F_{Tx}\cdot h_{FTx}}{L}$ fragment, we will see that the share of QE thrust action in the vehicle nosedive is inversely proportional to the wheelbase of the wheeled chassis of the quantomobile.

As for thrust, it loads the front wheels to the same extent as it unloads the rear wheels (see the signs of the last terms in Eqs. (3) and (4)).

With an increase in the vehicle weight, the nosedive effect is reduced: the increasing total weight G_q in the denominator of the k_{FTxn} complex reduces the value of this complex. However, in this case, we need to bear in mind that the vehicle load shifts the CoG height h_g, thus changing the values of the $k_{\psi n1}$, $k_{\psi n2}$ and k_{jn} complexes. It is obvious that lower values of the CoG height are required.

The issue of the longitudinal stability (neutralization of the overturning moment) of the quantomobile (as compared with the traditional vehicle) is becoming more acute. In automobiles, even the significant overturning moment is reflected (taken up) by the bearing surface (if there is a pressing force of the vehicle weight). In quantomobiles, thrust above the bearing surface creates a significant overturning impulse. Besides, quantomobile hovering (and even its breakoff from the bearing surface (Kotikov, 2019a, 2020)) requires assessment of this moment in order to neutralize negative angles of attack and eliminate the possibility of overturning.

Example. Let us consider a quantitative example of applying the introduced complexes when studying the longitudinal stability of the quantomobile and determining the value of the additional thruster to neutralize the overturning moment. We will examine a quantomobile with specifications similar to those of a KamAZ-4326 race truck considered in the previous studies (Kotikov, 2018a, 2018b, 2018c).

Let us restrict ourselves with a horizontal bearing surface. We will present calculations for the normal loads on the wheels of the front axle, bearing in mind that the load on the wheels of the rear axle at the perceived longitudinal overturning moment (with no vehicle hovering above the bearing surface) will be approximately equal to the difference between the total vehicle weight and the load on the wheels of the front axle. We will also neglect complex aerodynamics (shape of the vehicle body, air flows under the vehicle body, etc.) and use only the generalized aerodynamic coefficient.

To represent resistance against the rolling of the wheels, the following relationship was chosen: $f = f_{wh.0}(1 + f_{wh.V} \cdot V_q^2)$, where $f_{wh.0}$ – the coefficient of rolling resistance at the velocity close to zero (during starting), and $f_{wh.v}$ – the velocity coefficient of rolling resistance. Since the height of movement and air density are constant, the model of aerodynamic properties can be simplified: $c_x \cdot \rho/2 = k_{w.x}$.

Necessary data on the vehicle:

To perform a qualitative analysis, we chose a hypothetical quantomobile with the specifications of a similar KamAz-4326 automobile with a QE, under extremely severe conditions of motion: $G_q = 88$ kN; $f_{wh.0} = 0.3$; $f_{wh.V} = 4 \times 10^{-4}$ s^2/m^2; $k_{w.x} = 0.5$ N×s^2/m^4; $S_{front} = 7$ m^2; $\delta_{ric} = 0.04$ (Kotikov, 2019c).

Wheelbase L = 4,250 m; wheelbase components: L_1 = 2,100 m; L_2 = 2,150 m.

Height of force application (Figure 1): h_g = 1.3 m; h_w = 1.6 m; h_{FTx} = 1.0 m.

Maximum (implemented in the example in the entire velocity range) QE thrust value: 90 kN.

Let us use the graphic representation that was taken earlier for the quantomobile force balance analysis (Figure 2) (Kotikov, 2019a):

We used the following force balance equation for steady motion along a horizontal bearing surface:

$$P_x = \begin{pmatrix} f_{wh.0}(1 + f_{wh.v} \cdot V_q^2)) \cdot \\ G_q + k_{w.x} \cdot S_{front} \cdot V_x^2 \end{pmatrix}. \qquad (5)$$

The remainder of the force $F_{Tx} - P_x = P_a$ was used as the acceleration margin; at $F_{Tx.max} = G_q$, the corresponding area is highlighted in light green in Figure 2, and acceleration at $F_{Tx.max}$ is represented by the green *AB* line.

For $f_{wh.0}$ = 0.3, three zones are highlighted in Figure 2: wind resistance (blue), resistance of the bearing surface (yellow), vehicle acceleration margin (green). Figure 2 also shows the acceleration curve *AB* upon complete depletion of the thrust margin highlighted in green. It is possible to alter the zones for different values of $f_{wh.0}$ in a similar way.

Table 1 shows the results of calculating the complexes described above and presented in *Eq.* (3) for six velocity cross-sections of the quantomobile (Figure 2) at thrust F_{Tx} = 90 kN, accelerating from 0 to 67.2 m/s, which is the maximum velocity for this thrust value.

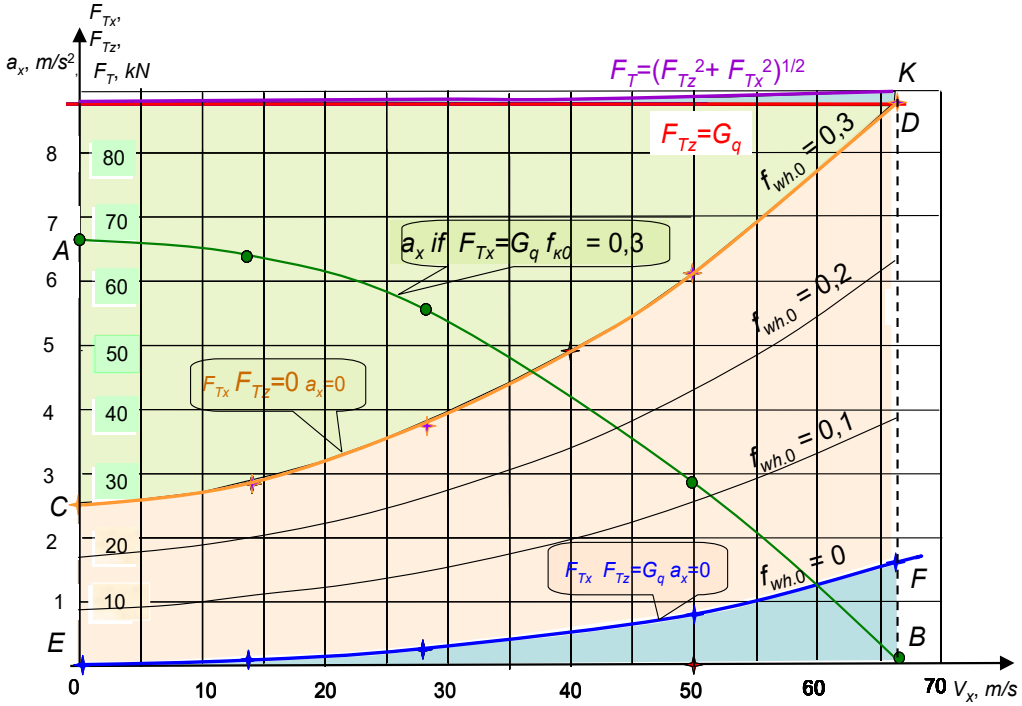

Figure 2. Quantomobile force balance when moving along the bearing surface with fwh.0 = 0.3 (fwh.0 = 0.1 and 0.2 — additionally)

Table 1. Calculated values of the linear complexes for different quantomobile acceleration points

State, velocity	Acceleration, m/s²	Complex $k_{\psi n1}$ components		Complexes, m				Location of the point of dynamic equilibrium
		L_2	$f{\cdot}r_d$	$k_{\psi n1}$	k_{wn}	k_{jn}	k_{FTxn}	$\sum k_i$, m
1. Standstill condition	0	2.15	0	2.15	0	0	0	2.15
2. Starting	6.7	2.15	–0.15	2.00	0	–0.923	1.023	2.10
3. 13.9 m/s	6.35	2.15	–0.17	1.98	–0.012	–0.876	1.023	2.115
4. 27.8 m/s	5.55	2.15	–0.20	1.95	–0.049	–0.765	1.023	2.159
5. 50.0 m/s	2.9	2.15	–0.31	1.84	–0.159	–0.400	1.023	2.304
6. 67.2 m/s	0	2.15	–0.43	1.72	–0.287	0	1.023	2.456

Table 1 shows that, for instance, at the maximum velocity, the point of dynamic equilibrium shifts at a distance of 2.456 – 2.15 = 0.306 m as compared with the position in the standstill condition.

If we shift to load units, the analysis may be just as informative. Let us transform Eq. (3) as follows:

The four obtained complexes have the force dimension and represent the share of each of them in the formation of the total normal load on the wheels of the same axle (let us call these force complexes). Table 2 shows the result of calculating these complexes for the same six vehicle states during acceleration.

$$\frac{G_q}{L}(k_{\psi n2} - k_{wn} - k_{jn} + k_{FTxn}) = R_{z\_\psi} - R_{z\_w} - R_{z\_j} + R_{z\_FTx}. \quad (6)$$

Table 2. Calculated values of the force complexes for different quantomobile acceleration points

State, velocity, m/s	Acceleration, m/s2	Load on the front axle in the standstill condition, kN	Share of the load from rolling resistance, kN	Contribution of the complexes in the normal load on the front wheels during longitudinal motion, kN				Load on the front wheels in motion, kN	Load on the rear wheels in motion, kN	Difference between the normal loads on the axles, kN	Overturning moment, kNm
		$R_{z1.\mathrm{st}}$	$\frac{f{\cdot}r_d}{G_q/L}$	R_{z_ψ}	R_{z_w}	R_{z_j}	$R_{z\_}F_{Tx}$	R_{z1}	R_{z2}	R_{z1}-R_{z2}	T_y
Standstill condition	0	44.5	0	0	0	0	0	44.5	43.5	1.0	4.25
Starting	6.7	44.5	–3.17	41.33	0	–19.1	21.19	43.42	44.58	–1.16	–4.93
13.9	6.35	44.5	–3.42	41.08	–0.25	–18.1	21.19	43.92	44.08	–0.16	–0.68
27.8	5.55	44.5	–4.14	40.36	–1.02	–15.8	21.19	44.73	43.27	1.46	6.20
50.0	2.9	44.5	–6.34	38.16	–3.29	–8.29	21.19	47.77	40.23	7.54	32.04
67.2	0	44.5	–8.88	35.62	–5.94	0	21.19	50.87	37.13	13.74	58.40

Table 2 shows that, with the velocity increase, the influence of rolling resistance $(f{\cdot}r_d)$ and wind resistance (R_{z_w}) on the formation of the normal loads on the wheels increases as well. The portion of the load on the wheels, caused by the inertial forces of the vehicle, decreases with the velocity increase (due to the acceleration decrease, see Figure 2).

The thrust of 90 kN, acting longitudinally on the vehicle body at a height h = 1 m (Figure 1), results in an increase in the normal reaction of the front wheels (R_{z_FTx} = 21.19 kN).

The load on the rear wheels R_{z2} can be calculated by using Eq. (4), but in the case of a horizontal bearing surface, the difference $R_{z2} = G_q - R_{z1}$ can be used.

The overturning moment is determined as follows: $T_y = (R_{z1} - R_{z2}) \cdot L$.

The maximum overturning moment T_y = 58.4 kNm occurs at a velocity of 67.2 m/s; this value is quite significant and should be neutralized. The simplest solution is to move the additional thruster having a vertical structure forward at a distance of 2.5 m from the point of dynamic equilibrium (see $\sum k_i$ = 2.456 in Table 1). To ensure stabilization, a force of 58.4 kNm / 2.5 m = 23.4 kN (one fourth of the force of the main thruster) will be required. Without stabilization, such imbalance will result in overturning when moving along a microprofile bearing surface. In the mode of partial or full hovering (Kotikov, 2020), the out-of-limit negative angle of attack will occur.

In the case of changes in the h_w, h_{FTx}, h_g heights (Figure 1) and their combinations, the nature of the contribution of the corresponding forces (and even their signs) in the formation of the normal loads will change as well. In this paper, we have just numerically demonstrated the methodical approach.

The fact that the example provided used the imperfect KamAZ-4326 body shape shows that it is possible to improve significantly the quantomobile aerodynamics and configure the vehicle in the shape of a flying wing (Stepanov, 1963). Then, at high speeds, due to emerging buoyancy, the normal reactions will be distributed in another way, with a decrease in the longitudinal overturning moment (or even its elimination). Nevertheless, the method developed can serve as the basis for further studies, quantomobile configuration design and implementation.

Conclusion

In this paper, we considered the diagram of forces acting on the quantomobile, including thrust generated by a QE (thruster) hovering above the bearing surface. A quantomobile shall have at least three thrusters to ensure not only the longitudinal motion in the pitch plane but roll and yaw control as well (Kotikov, 2018c). The diagram considered shall underlie the formation of multi-thruster diagrams for quantomobile motion and control.

References

Kotikov, Ju. (2018a). Comparative analysis of energy consumption by modern cars and future quantomobiles. *Architecture and Engineering,* Vol. 3, Issue 4, pp. 24–30. DOI: 10.23968/2500–0055–2018–3–4–24–30.

Kotikov, Ju. G. (2018b). Quantomobile: research of formation and imposition of thrust. Bulletin of Civil Engineers, No. 4 (69), pp. 189–198. DOI: 10.23968/1999–5571–2018–15–4–189–198.

Kotikov, Ju. G. (2018c). *Transport energetics: monograph.* Saint Petersburg: Saint Petersburg State University of Architecture and Civil Engineering, 206 p.

Kotikov, Ju. (2019a). Actualization of the quantomobile force balance in the pitch plane. *Architecture and Engineering,* Vol. 4, Issue 2, pp. 53–60. DOI: 10.23968/2500–0055–2019–4–2–53–60.

Kotikov, Ju. G. (2019b). Calculation research of the quantomobile power balance. *Bulletin of Civil Engineers,* No. 2 (73), pp. 147–152. DOI: 10.23968/1999–5571–2019–16–2–147–152.

Kotikov, Ju. (2019c). Graphical-and-analytical basis for quantomobile near-ground motion studies. *Architecture and Engineering,* Vol. 4, Issue 3, pp. 55–64. DOI: 10.23968/2500–0055–2019–4–3–55–64.

Kotikov, Ju. (2019d). Specifics of the quantomobile force balance. *Architecture and Engineering,* Vol. 4, Issue 1, pp. 3–10. DOI: 10.23968/2500–0055–2019–4–1–3–10.

Kotikov, Ju. G. (2019e). Traction-speed properties of the quantomobile. *Bulletin of Civil Engineers,* No. 1 (72), pp. 168–176. DOI: 10.23968/1999–5571–2019–16–1–168–176.

Kotikov, Ju. (2020). The rise of the quantomobile theory. *Architecture and Engineering,* Vol. 5, Issue 4, pp. 74–81. DOI: 10.23968/2500–0055–2020–5–4–74–81.

Leonov, V. S. (2002). *Method of creating thrust in vacuum and field engine for spacecraft (versions).* Patent No. RU2185526C1.

Leonov, V. S. (2010). *Quantum energetics. Vol. 1. Theory of Superunification.* Cambridge: Cambridge International Science Publishing, 745 p.

Selifonov, V. V., Khusainov, A. Sh. and Lomakin, V. V. (2007). *Automobile theory: study guide.* Moscow: Moscow State Technical University “MAMI”, 102 p.

Stepanov, G. Yu. (1963). *Hydrodynamic theory of air-cushion vehicles.* Moscow: Mashgiz, 94 p.

Volkov, Ye. V. (2018). *Car motion theory: monograph.* Khabarovsk: Publishing House of Pacific National University, 204 p.

РАСПРЕДЕЛЕНИЕ НОРМАЛЬНЫХ РЕАКЦИЙ НА КОЛЕСАХ КВАНТОМОБИЛЯ

Юрий Георгиевич Котиков

Санкт-Петербургский государственный архитектурно-строительный университет
2-ая Красноармейская ул., 4, Санкт-Петербург, Россия

E-mail: cotikov@mail.ru

Аннотация
Продвижение научно-технической мысли обозначило возможность создания квантовых двигателей (КвД), использующих энергию физического вакуума. КвД будет создавать векторную тяговую силу (траст), которую можно непосредственно, исключая трансмиссию, прикладывать к корпусу экипажа для его движения. Классический автомобиль при установке на нем КвД трансформируется в квантомобиль. Приложение силы тяги КвД (траста) в вывешенной над опорной поверхностью точке корпуса экипажа меняет традиционную схему сил, действующих на экипаж. Возникает необходимость оценки влияния действия траста на продольную устойчивость квантомобиля. **Методы:** Применен метод модернизации схемы сил, действующих на классический автомобиль, путем введения траста КвД, вывешенного над опорной поверхностью. Построена соответствующая математическая модель распределения нормальных реакций на колесах, учитывающая размещение КвД. **Результаты:** Среди сформированных расчетных комплексов для качественного анализа влияния силовых факторов на загрузку шасси квантомобиля выделен комплекс, представляющий продольную силу тяги и высоту расположения траста КвД. **Обсуждение:** Комплексы могут явиться основой расчетных блоков для более детализированного программирования, анализа и синтеза конструкции экипажа с КвД, оценки продольной устойчивости экипажа, оптимизации размещения КвД в корпусе квантомобиля. **Пример:** Демонстрация методики осуществлена на примере квантомобиля-аналога КамАЗ-4326. **Заключение:** Рассмотренная схема сил, действующих на квантомобиль, включающая тяговую силу КвД (траст), реализуемую над опорной поверхностью, должна стать родовой (generic) для формирования силовых схем квантомобилей с дополнительными трастерами для повышения продольной устойчивости экипажа.

Ключевые слова
Квантовый двигатель, квантомобиль, силовой баланс, нормальные реакции на колеса, продольная устойчивость.